Heterometallic Complexes Hot Paper

How to cite: *Angew. Chem. Int. Ed.* **2022,** *61,* e202209797
International Edition: doi.org/10.1002/anie.202209797
German Edition: doi.org/10.1002/ange.202209797

Towards Hexagonal Planar Nickel: A Dispersion-Stabilised Tri-Lithium Nickelate

Andryj M. Borys, Lorraine A. Malaspina, Simon Grabowsky, and Eva Hevia**

Abstract: Advancing the understanding of lithum nickelate complexes, here we report a family of homoleptic organonickelate complexes obtained by reacting Ni(COD)$_2$ and lithium aryl-acetylides in the presence of the bidentate donor TMEDA. These compounds represent rare examples of low-valent transition-metals supported solely by organolithium ligands. Whilst the solid-state structures indicate a hexagonal planar geometry around Ni^0 with Ni–Li bonds, bonding analysis via QTAIM, NCI, NBO and ELI methods reveals that the Ni–Li interactions are repulsive in nature, characterising these complexes as tri-coordinated. London dispersion forces between TMEDA and the organic substituents on nickel are found to play a crucial role in the stabilisation and thus isolation of these complexes. Preliminary reactivity studies demonstrate that the homoleptic lithium nickelates undergo stoichiometric cross-coupling with PhI to give dinickel clusters containing both anionic acetylide and neutral alkyne ligands.

Six-coordinate transition-metals adopting a hexagonal planar geometry, whilst known for polynuclear clusters,[1–3] condensed phases[4–6] or within the pores of coordination polymers,[7] are remarkably rare for discrete transition-metal complexes. Well-defined hexagonal planar palladium complexes were reported by Crimmin and co-workers in 2019,[8] and this has recently been extended to the platinum congener (**I**, Scheme 1a).[9] Prior to these studies, hexagonal planar nickel complexes such as [Ni(P^{t}Bu)$_6$] were reported,[10] however, subsequent theoretical studies revealed that these and related species are best described as trigonal planar complexes with a 16-electron count,[11] akin to classical Ni^0 *tris*-olefin compounds.[12,13] The bonding scenario in **I** is markedly different, however, as it combines

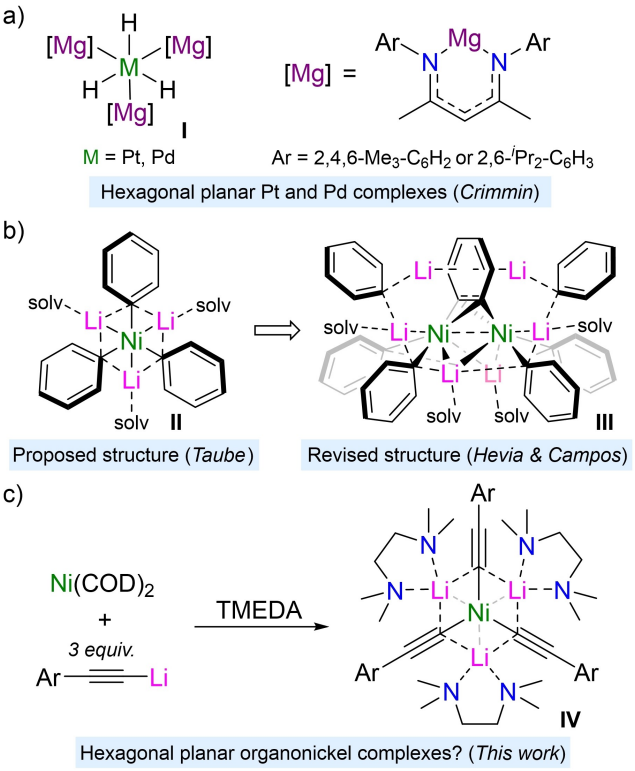

Scheme 1. Examples of hexagonal planar transition-metal complexes.

an alternating array of σ-donating (H$^-$) and σ-accepting (LMg$^+$) ligands, in which the M···Mg interactions are primarily ionic in nature.[8,9]

The overlooked tri-lithium nickelate "Li$_3$NiPh$_3$(solv)$_3$" (**II**, Scheme 1b), which possesses similar structural features to **I**, was documented by Taube in 1979.[14,15] Recently, however, we have reported that this proposed structure was misassigned and instead identified as an octanuclear cluster containing a bridging C$_6$H$_4$ ligand between two nickel centres, **III**.[16] Although Fe^0 complexes supported solely by phenyl-lithium ligands are known,[17] the isolation of **III** suggests that this is not possible for d^{10} Ni^0, leading to the *in situ* formation of the π-accepting, and formally reduced, C$_6$H$_4$ ligand in order to alleviate the extreme electron density at nickel. This hypothesis is further supported by the isolation of related side-on N$_2$ complexes obtained when treating Ni(CDT) (CDT = 1,5,9-cyclododecatriene) with an excess of PhLi or PhNa under an N$_2$ atmosphere.[18–20] Based on these findings, we reasoned that a carbanionic ligand which itself could serve as a suitable π-acceptor would

[*] Dr. A. M. Borys, Dr. L. A. Malaspina, PD Dr. S. Grabowsky, Prof. Dr. E. Hevia
Departement für Chemie, Biochemie und Pharmazie, Universität Bern
Freiestrasse 3, 3012 Bern (Switzerland)
E-mail: simon.grabowsky@unibe.ch
eva.hevia@unibe.ch

facilitate the synthesis and isolation of a hexagonal planar nickel complex (**IV**, Scheme 1c).

Treatment of $Ni(COD)_2$ (COD = 1,5-cyclooctadiene) with 3 equivalents of lithium phenyl-acetylide **1a** in the presence of a slight excess of bidentate donor TMEDA (TMEDA = *N,N,N′,N′*-tetramethylethylenediamine) afforded a deep purple reaction mixture which deposited the target complex $Li_3(TMEDA)_3Ni(C{\equiv}C{-}Ph)_3$ **2a** as a bronze microcrystalline solid in 81 % yield after filtration and washing (Figure 1a). This could be extended to other lithium aryl-acetylides to give **2b** (Ar = *p*-Tol) and **2c** (Ar = 3-thienyl) in 85 % and 28 % yield, respectively (see Supporting Information for details and solid-state structures). Akin to other alkali-metal nickelates that we have reported, the choice of solvent and donor is key to enabling their synthesis

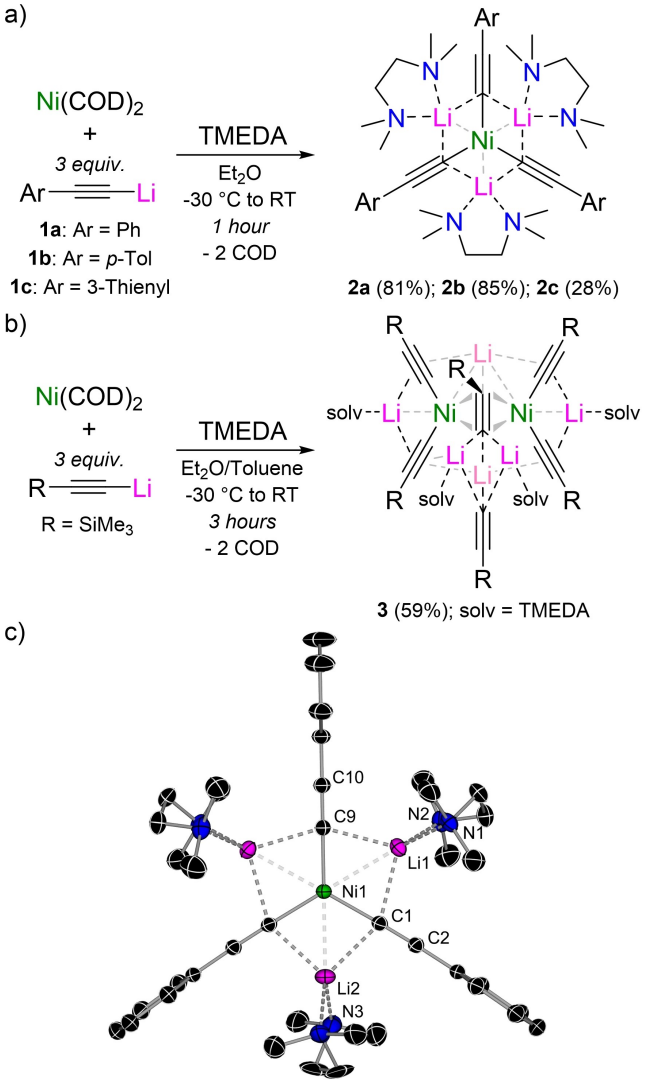

Figure 1. a) Synthesis of tri-lithium nickelates **2a–c**; b) Synthesis of lithium-nickelate cluster **3**; c) Molecular structure of **2a** shown with thermal ellipsoids at 30% probability. Hydrogen atoms and co-crystallised solvents omitted for clarity. Selected bond lengths (Å): Ni1–C9 1.856(2); Ni1–C1 1.8683(18); C9–C10 1.233(4); C1–C1 1.232(3); Ni1–Li1 2.512(3); Ni1–Li2 2.487(4); Li1–C9 2.264(4); Li1–C1 2.268(4); Li2–C1 2.228(4).

and isolation.[16,21,22] Et_2O and THF solvates of **2a** could not be isolated or spectroscopically observed, and the addition of 12-crown-4 to **2a** leads to immediate decomposition, illustrating that TMEDA plays an important role beyond lithium cation solvation (see below). Demonstrating the importance of the choice of alkynyl ligand, when using more electron-rich lithium acetylides such as $Me_3Si{-}C{\equiv}C{-}Li$ the polynuclear cluster $[Li_6(TMEDA)_{3.5}Ni_2(C{\equiv}C{-}SiMe_3)_6]_2$ (**3**) was formed (Figure 1b). This complex bears structural similarities to **III** in which a terminal lithium acetylide coordinates side-on between two nickel centres (see Supporting Information for experimental details and solid-state structure). Compounds **2a–c** are diamagnetic and show well-resolved ^1H, ^7Li and ^{13}C NMR spectra with signals in the expected range: for **2a** the acetylide signals are observed in the ^{13}C NMR spectrum at $\delta = 144.1$ and 100.7 ppm, respectively.[23]

The solid-state structure of **2a** (Figure 1c) shows an apparent six-coordinate, perfectly planar environment around Ni in which the TMEDA solvated lithium cations occupy sites nestled between the Ni-acetylides. The phenyl-substituents and TMEDA donors are orientated perpendicular to the planar core. The C–Ni–Li angles occupy a narrow range from 59.53(5)° to 60.25(10)°, consistent with a hexagonal planar geometry.[9] The Ni–C [Ni1–C1 1.8683 (18) Å; Ni1–C9 1.856(2) Å] and C≡C bond lengths [C1–C2 1.232(3) Å; C9–C10 1.233(4) Å] are comparable to reported low-valent nickel acetylides,[24] whilst the Li–C contacts [2.228(4)–2.267(4) Å] are typical for metalates containing TMEDA-solvated lithium acetylides.[25,26] The Ni–Li distances range from 2.487(4) Å to 2.512(3) Å which is within the sum of the covalent radii (2.52 Å)[27] and comparable to other lithium organonickelates derived from PhLi that we have reported containing TMEDA.[22] A Hirshfeld surface analysis[28] of **2a** (Figure 2a), in which red regions depict where contact distances between closest atoms below and above the surface are smaller than the sum of their van der Waals radii, further illustrates the existence of close contacts between Ni–Li and Li–C. In addition, there are red regions for close contacts significantly below the sum of atomic C and H van der Waals radii between the TMEDA methyl groups and the phenyl-acetylide substituents on nickel.

Since geometrical proximity is not necessarily an indicator of a bonding interaction, we further assessed the nature of the Ni–Li, Li–C and TMEDA-acetylide interactions and the overall bonding in **2a** by a complementary bonding analysis.[29] Isolated-molecule geometry optimisations of the entire complex **2a** were conducted at the B3LYP/def2-TZVP level of theory including empirical GD3BJ dispersion corrections.[30] A subsequent Quantum Theory of Atoms in Molecules (QTAIM)[31] topological analysis of the quantum-mechanical electron density yielded bond paths and corresponding bond critical points (bcps) for all Ni–C and Li–C interactions, but none for the Ni–Li contacts (Figure 2b). According to Bader, bond paths can be understood as bonding interactions—and the absence of bond paths as the absence of bonding interactions.[32] Hence, QTAIM presents the first indication of only a tri-coordinated nickel center despite the apparent Li proximity. The non-covalent inter-

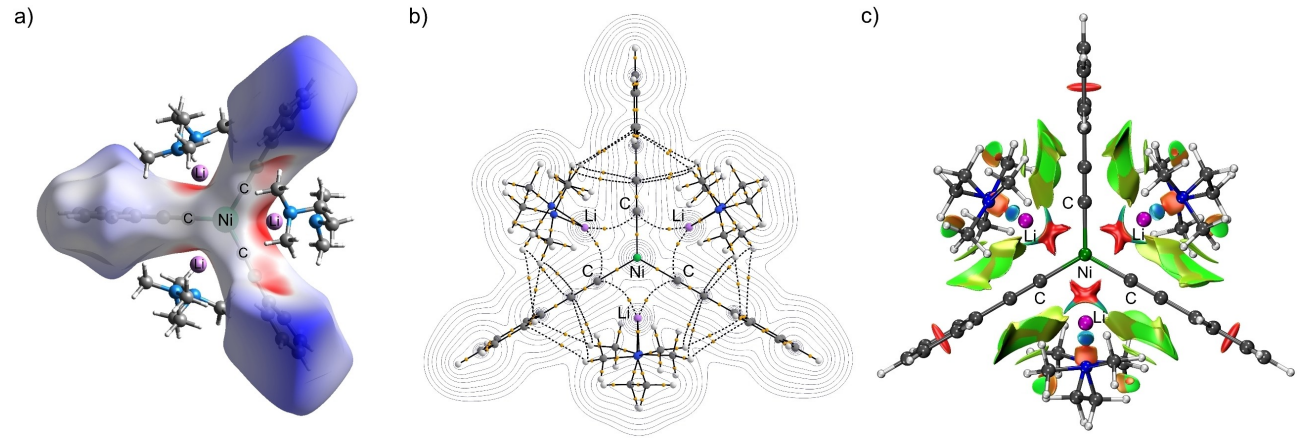

Figure 2. a) Hirshfeld surface analysis of **2a** with the property d_{norm} colour-coded onto it: Red = contact distance between closest atoms below and above the surface smaller than the sum of their van der Waals radii (ΣvdW); white = contact distance equal to ΣvdW; blue = contact distance larger than ΣvdW. b) Electron density contour map with the molecular graph according to QTAIM. Solid bond paths mean that there is high electron density at the corresponding bcps (orange balls); dashed means low electron density at the bcps. c) Isosurface representation of the reduced density gradient s (NCI index) at s(r) = 0.5 color coded with sign(λ_2)ρ: Red = repulsive; blue = attractive; green = weakly attractive.

action (NCI)[33] index clarifies the nature of the interactions as repulsive (red color), attractive (blue color) and weakly attractive (green-brown) (Figure 2c). It is striking that the forces prevailing along the Ni–Li axes are clearly repulsive, indicating that nickel is certainly not coordinated or bonded to lithium. Instead, in agreement with the bond paths motif, there are attractive interactions between the Li atoms and the C atoms of the acetylide substituents. These features contrast significantly to the hexagonal planar complexes reported by Crimmin (see **I**, Scheme 1a), which show QTAIM bond paths and attractive interactions (NCI plot) between the transition-metal (Pd, Pt) and s-block metal (Mg).[8,9]

Figures 2b and 2c also shed light on the interactions between the methyl groups of the TMEDA donor and the acetylide and phenyl carbon atoms of the C≡C–Ph ligands. Figure 2b shows various H···C bond paths in the electron density topology, whilst many broad NCI surfaces colored green between these groups are observed in Figure 2c. These represent attractive London dispersion (van der Waals) interactions,[34] and, although weak in nature, summed up over large areas of space they can significantly stabilise compounds to facilitate their isolation. In this optimised geometry, the sum of all Grimme-type terms between C≡C–Ph and TMEDA ligands amounts to 77.5 kJ mol^{-1}. If compared to the geometry obtained upon optimisation without GD3BJ empirical dispersion correction, this geometry is energetically more favorable by 754 kJ mol^{-1} mostly owing to some rearrangements in the TMEDA methyl groups. This striking importance of London dispersion acting between the ligands is supported experimentally by unsuccessful attempts to isolate or spectroscopically observe similar complexes with different Li cation donors such as Et_2O, THF or 12-crown-4 (see above). Hence, complexes **2a**–**c** are further examples in a row of recently discovered dispersion-stabilised molecules.[34–37]

The atomic NPA/QTAIM charges [NPA = natural population analysis, in the framework of natural bond orbital (NBO) analysis][38] for the Ni atom in **2a** are 0.33/0.30 e. The terminal-acetylide carbon atoms are negatively charged with −0.56/−0.41 e, with the remaining negative charges delocalised over the rest of the C≡C–Ph ligands. This shows that the overall direction of charge transfer is from the Ni atom towards the ligands, and that the Ni atom can only formally be described as a neutral Ni^0 center. The Li atoms are attracted electrostatically to the electron rich terminal C atoms of the acetylide groups (Figure 2c, blue extensions of the NCI surfaces attached to the red regions depicting Ni–Li repulsion), but in addition the reduced positive charge of the Li atoms (0.82/0.87e, NPA/QTAIM) indicates some minor orbital overlap with the C≡C π-system, which explains the occurrence of the Li···C bond paths in Figure 2b.

Significant back-bonding between the Ni atom and the acetylide unit is the mechanism behind the Ni→C charge transfer discussed in the previous paragraph. It can be depicted as a d-orbital (d_{xy} and $d_{x2\text{-}y2}$) to $\pi^*_{(C\equiv C)}$ interaction in NBO, as visualised in Figure 3a. Each of these Ni→C≡C–Ph back-bonding interactions (3 times) amounts to 48 kJ mol^{-1}, which is approximately a sixth of the energy of the forward σ-bonding interaction.[39] Back-bonding from the out-of-plane Ni d-orbitals (d_{xz} and d_{yz}) to the orthogonal $\pi^*_{(C\equiv C)}$ anti-bonding orbital is also observed, together with a weak back-bonding interaction from the Ni d_{z2} to $\sigma^*_{(C\equiv C)}$ orbital (see Figures S26–28). These non-Lewis backbonding perturbations stabilise the complex, but weakens the C≡C bond considerably; the bond orders are 2.36 (delocalisation index, DI)[40] or 2.56 (NLMO/NPA bond order; NLMO = natural localized molecular orbital, within NBO theory) instead of the expected 3.0. The loss in electrons of the C≡C bond can also be quantified using the Electron Localizability Indicator (ELI).[41] It indicates that there are only 4.6 instead of 6.0 electrons inside the bond basin of the formal triple bond (Figure 3b). The Ni–C bond orders are, in turn, 1.0 in both

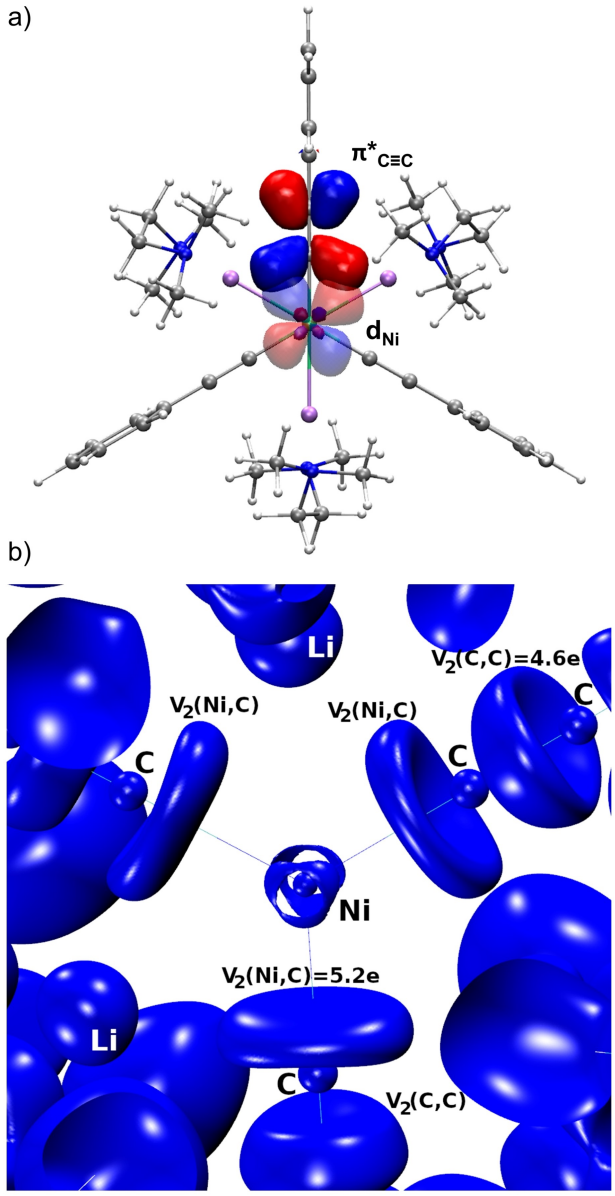

Figure 3. a) Visualisation of the overlap of the natural bond orbitals representing a Ni d-orbital and a C≡C antibonding π orbital. This non-Lewis contribution to bonding contributes a stabilisation energy (E2 energy) of 48 kJ mol^{-1}. b) ELI localisation domain representation at an isovalue of 1.40. The domains represent basins in ELI, disynaptic ones are labelled as V_2, and the total electron population of each Ni–C and C–C basin is given (they occur three times each).

DI and NLMO/NPA schemes. The electron distribution in the Ni–C interaction is more complex, though, because due to the back-bonding the entire 4s/3d–shell of the Ni atom has merged with the carbon lone pairs. This is visualised in Figure 3b by localisation domains representing disynaptic V_2(Ni,C) ELI basins which are populated with 5.2 e each (3 times). Note that the localisation domains are isosurface representations that only show the region around the source of the basin (the basins themselves are space-filling). This means that here the highest localisation of valence electrons is close to the C atoms and distant to the Ni atom. It is also noteworthy that the core–shell of the Ni atom (3s, 3p electrons) is polarised in the ligand field, reflecting its symmetry. Ligand induced charge localisations[42] alternate with depletions, and the latter point towards the highly populated C–Ni bond basins. Full details regarding the computations, software used and bonding analyses are given in the Supporting Information.

Thus, while based on the structural analysis it can be tempting to describe lithium nickelates **2a**–**c** as hexagonal planar organonickel complexes, careful analysis of the bonding present in these systems indicates that they are best described as trigonal planar species.

Having investigated the structure and bonding of the homoleptic tri-lithium nickelates, the reactivity of **2a** was explored. No reaction was observed with phosphines (PCy_3 or PEt_3) reflecting the quenched Lewis acidity at the nickel center. This is in stark contrast to the non-isolable nickel analogue of **I** (see Scheme 1a) which coordinates PCy_3 in the axial position to give a 7-coordinate hexagonal pyramidal complex.[8] However, compound **2a** reacts cleanly with one equivalent of iodobenzene to give hexanuclear cluster **4a** alongside diphenylacetylene and LiI (Figure 4a). Complex **4a** forms in 80 % spectroscopic yield from **2a** (see Figure S10) or can be independently prepared directly from $Ni(COD)_2$, Ph–C≡C–Li and Ph–C≡C–Ph (1:2:0.5 ratio) as

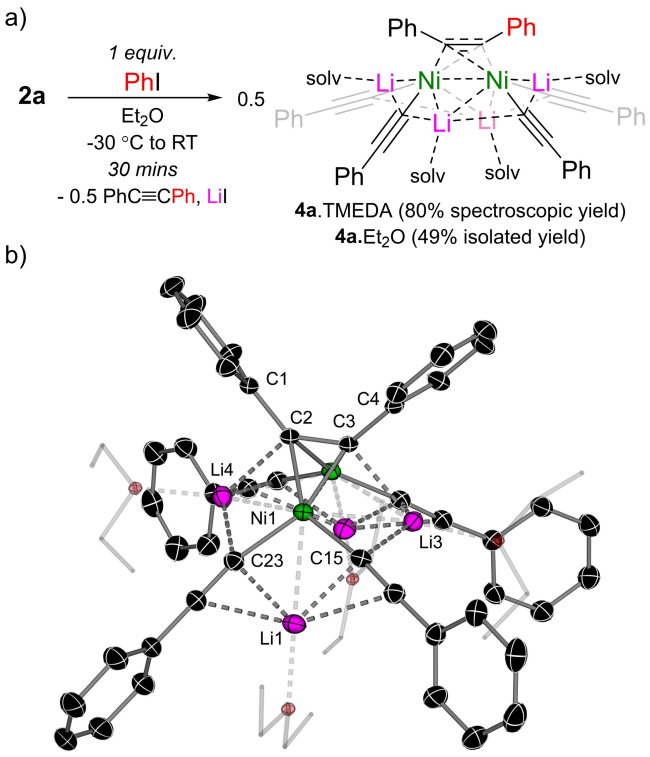

Figure 4. a) Synthesis of lithium nickelate **4a**; b) Molecular structure of **4a**.Et_2O shown with thermal ellipsoids at 30 % probability.[45] Hydrogen atoms omitted and ethyl groups of coordinated Et_2O shown as wireframe for clarity. Selected bond lengths (Å) and angles (°): C2–C3 1.371(2); Ni1–C2 1.937(1); Ni1–C3 1.972(1); Ni1–Ni2 2.6713(5); Ni1–C15 1.891(2); Ni1–C23 1.896(1); C2–Ni1–C3 41.05(5); C15–Ni1–C23 104.32(6).

the Et_2O solvate in 49 % crystalline yield. No further reaction is observed on the addition of excess iodobenzene, and complex **2a** cannot be regenerated by treatment of **4a** with Ph–C≡C–Li, rendering this system incapable of catalytic Sonogashira-type cross-coupling.[43]

The solid-state structure of **4a**.Et_2O (Figure 4b) adopts a distorted Li_4N_2 core in which diphenylacetylene coordinates side-on between two *pseudo*-trigonal planar nickel centres. This motif is reminiscent of that observed in the μ-η^2-η^2-C_6H_4 complex (**III**, see Scheme 1b)[16] and related N_2 complexes.[18–20] Elongation of the C2–C3 bond [1.371(2) Å; cf. 1.198(2) Å for Ph–C≡C–Ph][44] and bending away from linearity [C1–C2–C3 = 134.0(1)°] indicates significant back-donation from the electron-rich Ni centres, as previously observed for **III** (see Scheme 1b).[16] The C–Ni–C angles in **4a** are considerably narrower compared to **2a** [104.32(6)° for C23–Ni1–C15 in **4a** vs. 120.47(5)° for C9–Ni1–C1 in **2a**]. This leads to longer Ni···Li distances [range = 2.608(2) Å to 2.668(2) Å] which are outside the sum of the covalent radii (2.52 Å),[27] and contracted Li···C distances [range = 2.080(3) Å to 2.485(3) Å] including interactions with both carbon atoms of the acetylide π-system, a feature not observed in compounds **2a**–**c**.

In conclusion, we have demonstrated that homoleptic tri-lithium nickelates can be readily accessed from Ni(COD)$_2$ and lithium aryl-acetylides in the presence of TMEDA. Whilst interpretation of the bond lengths and angles implies a hexagonal planar geometry, complementary bonding analysis reveals that the Ni···Li interactions are repulsive, characterising these compounds as trigonal planar. Dispersion interactions between the Li-TMEDA units and the aryl-acetylide substituents were found to stabilise the compounds and thus facilitate their isolation. These results shed new light on the structure and bonding of hetero-bimetallic nickelate complexes, and show that for unusual compounds, geometrical analysis can be misleading and bonding analysis is crucial.

Acknowledgements

The Synergy diffractometer used for X-ray single crystal structure determination was partially funded by the Swiss National Science Foundation (SNSF) within the R′Equip programme (project number 206021_177033). We thank Dr. Ilche Gjuroski (NMR) and Andrea Bill (CHN) for analytical services, and Universität Bern and the SNSF (project grant 188573 to EH) for generous sponsorship of this research. Open access funding provided by Universität Bern. Open Access funding provided by Universität Bern.

Conflict of Interest

The authors declare no conflict of interest.

Data Availability Statement

The data that support the findings of this study are available in the supplementary material of this article.

Keywords: Complementary Bonding Analysis · London Dispersion · Nickel · Organolithium · Transition-Metal Complexes

[1] T. Yamada, A. Mawatari, M. Tanabe, K. Osakada, T. Tanase, *Angew. Chem. Int. Ed.* **2009**, *48*, 568–571; *Angew. Chem.* **2009**, *121*, 576–579.
[2] M. Tanabe, N. Ishikawa, M. Chiba, T. Ide, K. Osakada, T. Tanase, *J. Am. Chem. Soc.* **2011**, *133*, 18598–18601.
[3] A. W. Cook, P. Hrobárik, P. L. Damon, G. Wu, T. W. Hayton, *Inorg. Chem.* **2020**, *59*, 1471–1480.
[4] L. M. Yang, V. Bačić, I. A. Popov, A. I. Boldyrev, T. Heine, T. Frauenheim, E. Ganz, *J. Am. Chem. Soc.* **2015**, *137*, 2757–2762.
[5] R. N. Somaiya, Y. Sonvane, S. K. Gupta, *Comput. Mater. Sci.* **2020**, *173*, 109414.
[6] Y. Wang, Y. Li, Z. Chen, *Acc. Chem. Res.* **2020**, *53*, 887–895.
[7] Z. Niu, J. G. Ma, W. Shi, P. Cheng, *Chem. Commun.* **2014**, *50*, 1839–1841.
[8] M. Garçon, C. Bakewell, G. A. Sackman, J. P. Andrew, R. I. Cooper, A. J. Edwards, M. R. Crimmin, *Nature* **2019**, *574*, 390–396.
[9] A. Phanopolous, G. A. Sackman, C. Richardson, A. J. P. White, R. I. Cooper, A. J. Edwards, M. R. Crimmin, *ChemRxiv.* **2022**, https://doi.org/10.26434/chemrxiv-2022-t4wz6-v2.
[10] R. Ahlrichs, D. Fenske, H. Oesen, U. Schneider, *Angew. Chem. Int. Ed. Engl.* **1992**, *31*, 323–326; *Angew. Chem.* **1992**, *104*, 312–314.
[11] H. Tang, D. M. Hoffman, T. A. Albright, H. Deng, R. Hoffmann, *Angew. Chem. Int. Ed. Engl.* **1993**, *32*, 1616–1618.
[12] K. Fischer, K. Jonas, G. Wilke, *Angew. Chem. Int. Ed. Engl.* **1973**, *12*, 565–566; *Angew. Chem.* **1973**, *85*, 620–621.
[13] K. Jonas, P. Heimbach, G. Wilke, *Angew. Chem. Int. Ed. Engl.* **1968**, *7*, 949–950; *Angew. Chem.* **1968**, *80*, 1033–1033.
[14] R. Taube, N. Stransky, *Z. Chem.* **1979**, *19*, 412–413.
[15] R. Taube, *Comments Inorg. Chem.* **1984**, *3*, 69–81.
[16] R. J. Somerville, A. M. Borys, M. Perez-Jimenez, A. Nova, D. Balcells, L. A. Malaspina, S. Grabowsky, E. Carmona, E. Hevia, J. Campos, *Chem. Sci.* **2022**, *13*, 5268–5276.
[17] T. A. Bazhenova, R. M. Lobkovskaya, R. P. Shibaeva, A. E. Shilov, A. K. Shilova, M. Gruselle, G. Leny, B. Tchoubar, *J. Organomet. Chem.* **1983**, *244*, 265–272.
[18] K. Jonas, *Angew. Chem. Int. Ed. Engl.* **1973**, *12*, 997–998; *Angew. Chem.* **1973**, *85*, 1050–1050.
[19] C. Krüger, Y.-H. Tsay, *Angew. Chem. Int. Ed. Engl.* **1973**, *12*, 998–999; *Angew. Chem.* **1973**, *85*, 1051–1052.
[20] K. Jonas, D. J. Brauer, C. Krüger, P. J. Roberts, Y.-H. Tsay, *J. Am. Chem. Soc.* **1976**, *98*, 74–81.
[21] A. M. Borys, E. Hevia, *Organometallics* **2021**, *40*, 442–447.
[22] A. M. Borys, E. Hevia, *Angew. Chem. Int. Ed.* **2021**, *60*, 24659–24667; *Angew. Chem.* **2021**, *133*, 24864–24872.
[23] H. F. Klein, A. Petermann, *Inorg. Chim. Acta* **1997**, *261*, 187–195.
[24] J. M. Goicoechea, S. C. Sevov, *J. Am. Chem. Soc.* **2006**, *128*, 4155–4161.
[25] W. Clegg, J. García-Álvarez, P. García-Álvarez, D. V. Graham, R. W. Harrington, E. Hevia, A. R. Kennedy, R. E. Mulvey, L. Russo, *Organometallics* **2008**, *27*, 2654–2663.
[26] H. Kawaguchi, K. Tatsumi, *Organometallics* **1995**, *14*, 4294–4299.

[27] B. Cordero, V. Gómez, A. E. Platero-Prats, M. Revés, J. Echeverría, E. Cremades, F. Barragán, S. Alvarez, *Dalton Trans.* **2008**, 2832–2838.
[28] M. A. Spackman, D. Jayatilaka, *CrystEngComm* **2009**, *11*, 19–32.
[29] Complementary bonding analysis refers to a collection of methods in which both real space and Hilbert space are used together. S. Grabowsky, *Complementary Bonding Analysis*, De Gruyter, Berlin, **2021**.
[30] S. Grimme, S. Ehrlich, L. Goerigk, *J. Comput. Chem.* **2011**, *32*, 1456–1465.
[31] R. F. W. Bader, *Atoms in Molecules: A Quantum Theory*, Clarendon Press, Oxford, **1995**.
[32] R. F. W. Bader, *J. Phys. Chem. A* **2009**, *113*, 10391–10396.
[33] E. R. Johnson, S. Keinan, P. Mori-Sánchez, J. Contreras-García, A. J. Cohen, W. Yang, *J. Am. Chem. Soc.* **2010**, *132*, 6498–6506.
[34] J. P. Wagner, P. R. Schreiner, *Angew. Chem. Int. Ed.* **2015**, *54*, 12274–12296; *Angew. Chem.* **2015**, *127*, 12446–12471.
[35] D. J. Liptrot, P. P. Power, *Nat. Chem. Rev.* **2017**, *1*, 0004.
[36] K. L. Mears, C. R. Stennett, J. C. Fettinger, P. Vasko, P. P. Power, *Angew. Chem. Int. Ed.* **2022**, *61*, e202201318; *Angew. Chem.* **2022**, *134*, e202201318.
[37] S. Rösel, H. Quanz, C. Logemann, J. Becker, E. Mossou, L. Cañadillas-Delgado, E. Caldeweyher, S. Grimme, P. R. Schreiner, *J. Am. Chem. Soc.* **2017**, *139*, 7428–7431.
[38] F. Weinhold, C. R. Landis, *Discovering Chemistry with Natural Bond Orbitals*, Wiley, Hoboken, **2012**.
[39] If we artificially consider the main Lewis structure as having a lone pair at the acetylide carbon atom and not a sigma bond, then there is donation of this lone pair to the Ni Rydberg orbitals of $\approx$285 kJ mol^{-1} per acetylide ligand. Note that this is only an estimate of the forward sigma bonding energy within NBO theory.
[40] R. F. W. Bader, M. E. Stephens, *J. Am. Chem. Soc.* **1975**, *97*, 7391–7399.
[41] M. Kohout, *Int. J. Quantum Chem.* **2004**, *97*, 651–658.
[42] R. Pal, S. Mebs, M. W. Shi, D. Jayatilaka, J. M. Krzeszczakowska, L. A. Malaspina, M. Wiecko, P. Luger, M. Hesse, Y. S. Chen, J. Beckmann, S. Grabowsky, *Inorg. Chem.* **2018**, *57*, 4906–4920.
[43] R. Chinchilla, C. Nájera, *Chem. Rev.* **2007**, *107*, 874–922.
[44] M. Bolte, *CSD Commun.* **2012**, https://doi.org/10.5517/ccxmqs0.
[45] Deposition Numbers 2180282 (for **2a**), 2180283 (for **2b**), 2180284 (for **2c**), 2180285 (for **3**), 2180286 (for **4a**), 2083516 (for **4a**) contain the supplementary crystallographic data for this paper. These data are provided free of charge by the joint Cambridge Crystallographic Data Centre and Fachinformationszentrum Karlsruhe Access Structures service.

Manuscript received: July 5, 2022
Accepted manuscript online: August 3, 2022
Version of record online: August 24, 2022